Solvable Models in Ultracold Physics IV

Itzhak Roditi

Centro Brasileiro de Pesquisas Físicas

Rio de Janeiro, Brasil

August, 2014

2-site Bose-Hubbard

The Hamiltonian is given by

$$H = \frac{k}{8}(N_1 - N_2)^2 - \frac{\Delta\mu}{2}(N_1 - N_2) - \frac{\mathcal{E}_{\mathcal{J}}}{2}(b_1^\dagger b_2 + b_2^\dagger b_1). \quad (1)$$

2-site Bose-Hubbard

The Hamiltonian is given by

$$H = \frac{k}{8}(N_1 - N_2)^2 - \frac{\Delta\mu}{2}(N_1 - N_2) - \frac{\mathcal{E}_{\mathcal{J}}}{2}(b_1^\dagger b_2 + b_2^\dagger b_1). \quad (1)$$

- $b_1^\dagger, b_2^\dagger$ denote single-particle creation operators in two wells.

2-site Bose-Hubbard

The Hamiltonian is given by

$$H = \frac{k}{8}(N_1 - N_2)^2 - \frac{\Delta\mu}{2}(N_1 - N_2) - \frac{\mathcal{E}_{\mathcal{J}}}{2}(b_1^\dagger b_2 + b_2^\dagger b_1). \quad (1)$$

- $b_1^\dagger, b_2^\dagger$ denote single-particle creation operators in two wells.
- $N_1 = b_1^\dagger b_1, N_2 = b_2^\dagger b_2$ are the corresponding boson number operators.

2-site Bose-Hubbard

The Hamiltonian is given by

$$H = \frac{k}{8}(N_1 - N_2)^2 - \frac{\Delta\mu}{2}(N_1 - N_2) - \frac{\mathcal{E}_{\mathcal{J}}}{2}(b_1^\dagger b_2 + b_2^\dagger b_1). \quad (1)$$

- $b_1^\dagger, b_2^\dagger$ denote single-particle creation operators in two wells.
- $N_1 = b_1^\dagger b_1, N_2 = b_2^\dagger b_2$ are the corresponding boson number operators.
- The total boson number $N_1 + N_2$ is conserved and set to the fixed value of N.

2-site Bose-Hubbard

The Hamiltonian is given by

$$H = \frac{k}{8}(N_1 - N_2)^2 - \frac{\Delta\mu}{2}(N_1 - N_2) - \frac{\mathcal{E}_{\mathcal{J}}}{2}(b_1^\dagger b_2 + b_2^\dagger b_1). \quad (1)$$

- $b_1^\dagger, b_2^\dagger$ denote single-particle creation operators in two wells.
- $N_1 = b_1^\dagger b_1, N_2 = b_2^\dagger b_2$ are the corresponding boson number operators.
- The total boson number $N_1 + N_2$ is conserved and set to the fixed value of N.
- The coupling k provides the strength of the scattering interaction between bosons

2-site Bose-Hubbard

The Hamiltonian is given by

$$H = \frac{k}{8}(N_1 - N_2)^2 - \frac{\Delta\mu}{2}(N_1 - N_2) - \frac{\mathcal{E}_{\mathcal{J}}}{2}(b_1^\dagger b_2 + b_2^\dagger b_1). \quad (1)$$

- $b_1^\dagger, b_2^\dagger$ denote single-particle creation operators in two wells.
- $N_1 = b_1^\dagger b_1, N_2 = b_2^\dagger b_2$ are the corresponding boson number operators.
- The total boson number $N_1 + N_2$ is conserved and set to the fixed value of N.
- The coupling k provides the strength of the scattering interaction between bosons
- $\Delta\mu$ is the external potential and $\mathcal{E}_J$ is the coupling for the tunneling.

2-site Bose-Hubbard

The Hamiltonian is given by

$$H = \frac{k}{8}(N_1 - N_2)^2 - \frac{\Delta\mu}{2}(N_1 - N_2) - \frac{\mathcal{E}_{\mathcal{J}}}{2}(b_1^\dagger b_2 + b_2^\dagger b_1). \quad (1)$$

- $b_1^\dagger, b_2^\dagger$ denote single-particle creation operators in two wells.
- $N_1 = b_1^\dagger b_1, N_2 = b_2^\dagger b_2$ are the corresponding boson number operators.
- The total boson number $N_1 + N_2$ is conserved and set to the fixed value of N.
- The coupling k provides the strength of the scattering interaction between bosons
- $\Delta\mu$ is the external potential and $\mathcal{E}_J$ is the coupling for the tunneling.
- The change $\mathcal{E}_J \to -\mathcal{E}_J$ corresponds to the unitary transformation $b_1 \to b_1$, $b_2 \to -b_2$, while $\Delta\mu \to -\Delta\mu$ corresponds to $b_1 \leftrightarrow b_2$.

Therefore we will restrict our analysis to the case of $\mathcal{E}_J$, $\Delta\mu \geq 0$. For $k > 0$, it is useful to divide the parameter space into three regimes;

Therefore we will restrict our analysis to the case of $\mathcal{E}_J$, $\Delta\mu \geq 0$. For $k > 0$, it is useful to divide the parameter space into three regimes;

- Rabi ($k/\mathcal{E}_J << N^{-1}$),

Therefore we will restrict our analysis to the case of $\mathcal{E}_J$, $\Delta\mu \geq 0$. For $k > 0$, it is useful to divide the parameter space into three regimes;

- Rabi ($k/\mathcal{E}_J << N^{-1}$),
- Josephson ($N^{-1} << k/\mathcal{E}_J << N$)

Therefore we will restrict our analysis to the case of $\mathcal{E}_J$, $\Delta\mu \geq 0$. For $k > 0$, it is useful to divide the parameter space into three regimes;

- Rabi ($k/\mathcal{E}_J << N^{-1}$),
- Josephson ($N^{-1} << k/\mathcal{E}_J << N$)
- and Fock ($N << k/\mathcal{E}_J$).

For these three regimes, there is a correspondence between the Hamiltonian (1) and the motion of a pendulum (Legget RMP 2001).

Therefore we will restrict our analysis to the case of $\mathcal{E}_J$, $\Delta\mu \geq 0$. For $k > 0$, it is useful to divide the parameter space into three regimes;

- Rabi ($k/\mathcal{E}_J << N^{-1}$),
- Josephson ($N^{-1} << k/\mathcal{E}_J << N$)
- and Fock ($N << k/\mathcal{E}_J$).

For these three regimes, there is a correspondence between the Hamiltonian (1) and the motion of a pendulum (Legget RMP 2001).

- In the Rabi and Josephson regimes this motion is semiclassical, in contrast to the Fock regime.

Therefore we will restrict our analysis to the case of $\mathcal{E}_J$, $\Delta\mu \geq 0$. For $k > 0$, it is useful to divide the parameter space into three regimes;

- Rabi ($k/\mathcal{E}_J << N^{-1}$),
- Josephson ($N^{-1} << k/\mathcal{E}_J << N$)
- and Fock ($N << k/\mathcal{E}_J$).

For these three regimes, there is a correspondence between the Hamiltonian (1) and the motion of a pendulum (Legget RMP 2001).

- In the Rabi and Josephson regimes this motion is semiclassical, in contrast to the Fock regime.
- For both the Fock and Josephson regimes the analogy corresponds to a pendulum with fixed length,

Therefore we will restrict our analysis to the case of $\mathcal{E}_J$, $\Delta\mu \geq 0$. For $k > 0$, it is useful to divide the parameter space into three regimes;

- Rabi ($k/\mathcal{E}_J << N^{-1}$),
- Josephson ($N^{-1} << k/\mathcal{E}_J << N$)
- and Fock ($N << k/\mathcal{E}_J$).

For these three regimes, there is a correspondence between the Hamiltonian (1) and the motion of a pendulum (Legget RMP 2001).

- In the Rabi and Josephson regimes this motion is semiclassical, in contrast to the Fock regime.
- For both the Fock and Josephson regimes the analogy corresponds to a pendulum with fixed length,
- while in the Rabi regime the length varies.

Classical dynamics

Let us study a classical analogue of the model. Let N_j, θ_j, $j = 1, 2$ be quantum variables satisfying the canonical relations

$$[\theta_1, \theta_2] = [N_1, N_2] = 0, \qquad [N_j, \theta_k] = i\delta_{jk} I.$$

Classical dynamics

Let us study a classical analogue of the model. Let N_j, θ_j, $j = 1, 2$ be quantum variables satisfying the canonical relations

$$[\theta_1, \theta_2] = [N_1, N_2] = 0, \qquad [N_j, \theta_k] = i\delta_{jk} I.$$

Using

$$\exp(i\theta_j) N_j = (N_j + 1) \exp(i\theta_j)$$

Classical dynamics

Let us study a classical analogue of the model. Let N_j, θ_j, $j = 1, 2$ be quantum variables satisfying the canonical relations

$$[\theta_1, \theta_2] = [N_1, N_2] = 0, \qquad [N_j, \theta_k] = i\delta_{jk} I.$$

Using

$$\exp(i\theta_j) N_j = (N_j + 1) \exp(i\theta_j)$$

we make a change of variables from the operators b_j, $b_j^\dagger$, $j = 1, 2$ via

$$b_j = \exp(i\theta_j)\sqrt{N_j}, \quad b_j^\dagger = \sqrt{N_j} \exp(-i\theta_j)$$

such that the Heisenberg canonical commutation relations are preserved.

Classical dynamics

Let us study a classical analogue of the model. Let N_j, θ_j, $j = 1, 2$ be quantum variables satisfying the canonical relations

$$[\theta_1, \theta_2] = [N_1, N_2] = 0, \qquad [N_j, \theta_k] = i\delta_{jk} I.$$

Using

$$\exp(i\theta_j) N_j = (N_j + 1) \exp(i\theta_j)$$

we make a change of variables from the operators b_j, $b_j^\dagger$, $j = 1, 2$ via

$$b_j = \exp(i\theta_j)\sqrt{N_j}, \quad b_j^\dagger = \sqrt{N_j} \exp(-i\theta_j)$$

such that the Heisenberg canonical commutation relations are preserved.Next define the variables

$$z = (N_1 - N_2)/N$$

$$\phi = N(\phi_1 - \phi_2)/2$$

where z represents the fractional occupation difference (or the *imbalance*) and ϕ the phase difference.

Classical limit

In the classical limit where N is large, but still finite, we may equivalently consider the Hamiltonian

$$H(z,\phi) = \frac{\mathcal{E}_J N}{2}\left(\frac{\lambda}{2}z^2 - \beta z - \sqrt{1-z^2}\cos(2\phi/N)\right) \tag{2}$$

where

$$\lambda = \frac{kN}{2\mathcal{E}_J}, \qquad \beta = \frac{\Delta\mu}{\mathcal{E}_J}$$

and $(z,\,\phi)$ are canonically conjugate variables. We note the Hamiltonian (2) obeys the symmetries

$$\begin{aligned} H\left(z,\phi\right)|_{\lambda,\beta} &= -\,H\left(z,\phi+N\pi/2\right)|_{-\lambda,-\beta} \\ H\left(z,\phi\right)|_{\lambda,\beta} &= H\left(-z,\phi\right)|_{\lambda,-\beta}\,. \end{aligned} \tag{3}$$

The classical dynamics is given by Hamilton's equations of motion

$$\begin{aligned} \dot{\phi} &= \frac{\partial H}{\partial z} = \frac{\mathcal{E}_J N}{2}\left(\lambda z - \beta + \frac{z}{\sqrt{1-z^2}}\cos(2\phi/N)\right) \\ \dot{z} &= -\frac{\partial H}{\partial \phi} = -\mathcal{E}_J\left(\sqrt{1-z^2}\sin(2\phi/N)\right). \end{aligned} \tag{4}$$

Now we study the fixed points of the Hamiltonian (2), determined by the condition $\dot{z} = \dot{\phi} = 0$.

This leads to the following classification:

- $\phi = 0$ and z is a solution of

$$\lambda z - \beta = -\frac{z}{\sqrt{1-z^2}} \tag{5}$$

  which has a unique real solution for $\lambda > 0$.

- $\phi = N\pi/2$ and z is a solution of

$$\lambda z - \beta = \frac{z}{\sqrt{1-z^2}}. \tag{6}$$

  This equation has either one, two or three real solutions for $\lambda > 0$.

From eq. (6) we can determine that there are fixed point bifurcations for certain choices of the coupling parameters.

From eq. (6) we can determine that there are fixed point bifurcations for certain choices of the coupling parameters.These bifurcations allow us to divide the coupling parameter space in two regions.

From eq. (6) we can determine that there are fixed point bifurcations for certain choices of the coupling parameters.These bifurcations allow us to divide the coupling parameter space in two regions. Setting $f(z) = \lambda z - \beta$ and $g(z) = z(1 - z^2)^{-1/2}$, the boundary between the regions occurs when $f(z)$ is the tangent line to $g(z)$ at some value z_0.
It is possible to verify that this occurs when $\lambda = g'(z_0) = (1 - z_0^2)^{-3/2}$. Requiring $f(z_0) = g(z_0)$ then yields the following relationship

$$\lambda = (1 + |\beta|^{2/3})^{3/2} \tag{7}$$

determining the boundary. This is depicted next in Fig. 1.

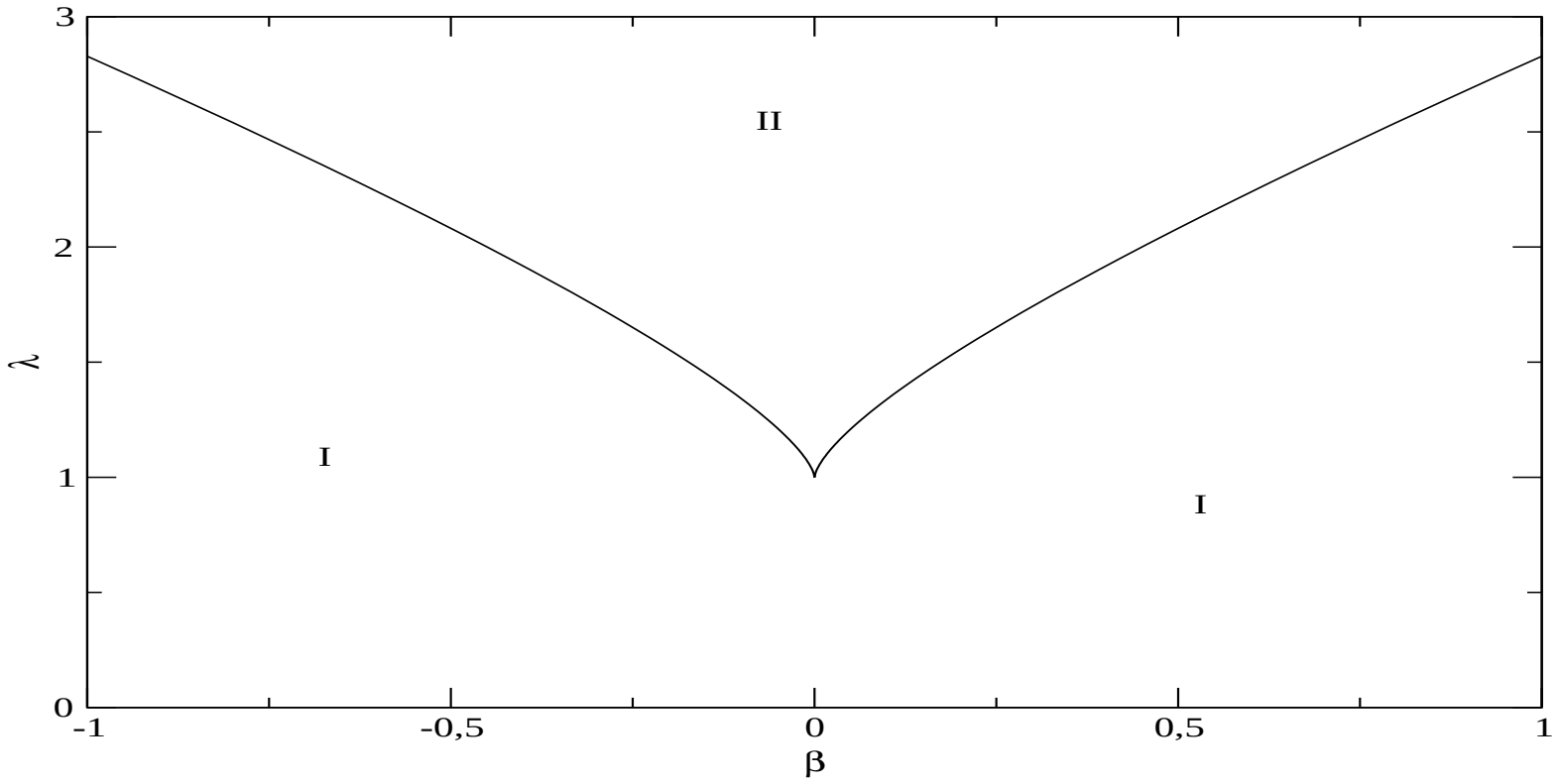

Figure: Coupling parameter space diagram identifying the different types of solutions for equation (6). In region I there is just one solution for z, a local maximum. In region II there are three solutions for z, two local maxima and a saddle point. The boundary separating regions I and II is given by (7).

This leads us to the following classification:

- $0 < \lambda < 1$: For any value of β there is just one real solution, for which the Hamiltonian attains a local maximum.
- $\lambda > 1$: Here transition couplings $\pm\beta_0$ appear, which can be seen from Fig. 1. For $\beta \in (-\beta_0, \beta_0)$, the equation has two locally maximal fixed points and one saddle point, while for $\beta > \beta_0$ or $\beta < -\beta_0$ the equation has just one real solution, a locally maximal fixed point.

We remark that in the absence of the external potential ($\Delta\mu = \beta = 0$) the transition value is given by $\lambda_0 = 1$. Using the symmetry relation (3) we can deduce that for the attractive case $\lambda < 0$, $\lambda_0 = -1$ is the coupling marking a bifurcation between a locally minimal fixed point (for $\lambda > -1$) and two locally minimal fixed points and a saddle point (for $\lambda < -1$). This is a supercritical pitchfork bifurcation of the classical ground state. Hines et al. (PRA 2005) predict that the ground-state entanglement, as measured by the von Neumann entropy, is maximal at this coupling. Pan and Dryer (PLA 2005) confirmed this result numerically.

Next we look at the dynamical evolution. In that which follows we will consider the equations (4) in the absence of the external field ($\Delta\mu = 0$ or, equivalently, $\beta = 0$). An analysis including the effect of this term can be found in the literature. We integrate (4) to find the time evolution for the imbalance z, using the initial condition $z(0) = 1$, $\phi(0) = 0$. By plotting z against the time, it is evident that there is a threshold coupling $\lambda_c = 2$ separating two different behaviors in the classical dynamics, as can be seen in Fig. 2:

(i) For $\lambda < 2$ the system oscillates between $z = -1$ and $z = 1$. Here the evolution is delocalized;

(ii) For $\lambda > 2$ the system oscillates between $z = 0$ and $z = 1$. Here the evolution is localized.

The threshold occurring at $\lambda_c = 2$ was first observed by Milburn et al.

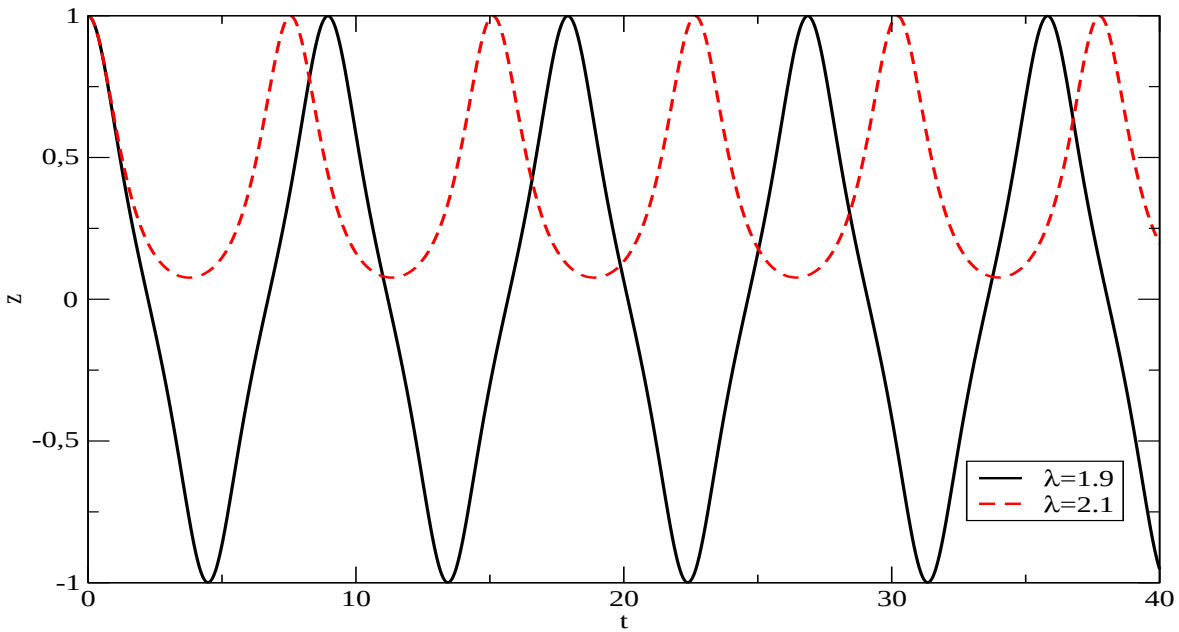

Figure: Time evolution for the imbalance z. The solid line is for $\lambda = 1.9$, while the dashed curve is for $\lambda = 2.1$. Here we are using $N = 100$, $\mathcal{E}_J = 1$ and the initial conditions $z(0) = 1$, $\phi(0) = 0$. The threshold coupling occurs at $\lambda_c = 2$.

To help visualize the classical dynamics, it is useful to plot the level curves (constant energy curves) of the Hamiltonian (2) in phase space. Given an initial condition $(z(0), \phi(0))$, the system follows a trajectory along the level curve $H(z(0), \phi(0))$. In Fig. 3 we plot the level curves for different values of λ ($\lambda = 1.5$ on the left and $\lambda = 2.5$ on the right), where we take $2\phi/N \in [-\pi, \pi]$. We can observe clearly two distinct scenarios:

- $\lambda > 2$: Here we see that for the orbit with initial condition $z_0 = 1$, $\phi(0) = 0$, ϕ increases monotonically (running phase mode). The evolution of z is bounded in the interval $[0, 1]$, leading to localization (self-trapping).
- $\lambda < 2$: Here we see that for the orbit with initial condition $z(0) = 1$, $\phi(0) = 0$, the evolution of ϕ is oscillatory and bounded in the interval $(-N\pi/2, N\pi/2)$. The evolution of z is not bounded, leading to delocalization.

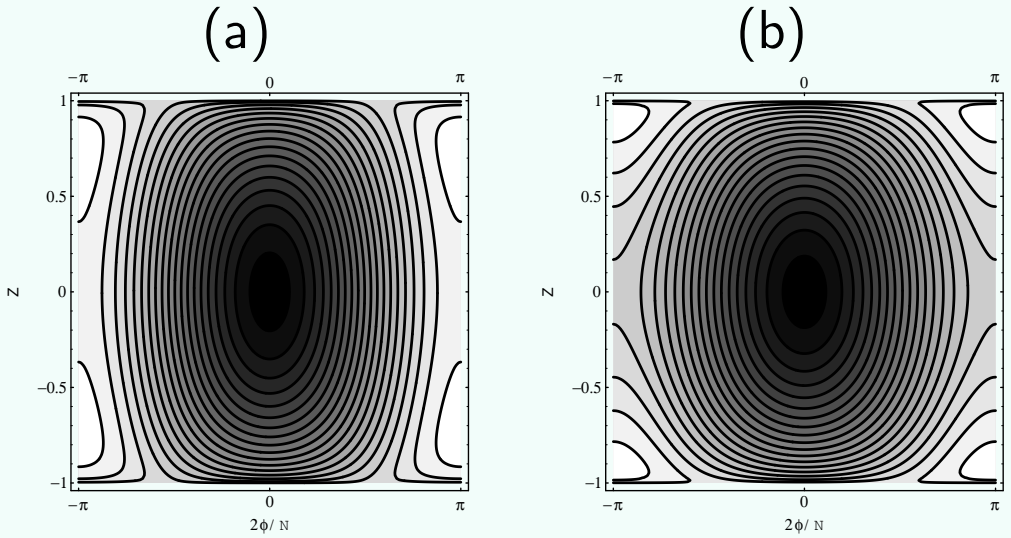

Figure: Level curves of the Hamiltonian (2) (a) for $\lambda = 1.5$ (below the threshold point) and (b) for $\lambda = 2.5$ (above the threshold point). We are using $N = 100$ and $\mathcal{E}_J = 1$. Above the threshold coupling running phase modes occur leading to localized evolution of z. Below the threshold coupling the evolution of z is delocalized.

The threshold coupling $\lambda_c = 2$ (or $k/\mathcal{E}_{\mathcal{J}} = 4/N$, in terms of the original variables) separates two distinct dynamical behaviors. This value for the threshold between delocalization and self-trapping also occurs for the quantum dynamics, as we will show in the next slide.

Quantum dynamics

One can investigate the quantum dynamics of the Hamiltonian in the absence of the external potential ($\Delta\mu = 0$) using the exact diagonalization method.
The time evolution of any state is determined by

$$|\Psi(t)\rangle = U(t)|\phi_0\rangle,$$

Quantum dynamics

One can investigate the quantum dynamics of the Hamiltonian in the absence of the external potential ($\Delta\mu = 0$) using the exact diagonalization method.
The time evolution of any state is determined by

$$|\Psi(t)\rangle = U(t)|\phi_0\rangle,$$

where U is the temporal evolution operator given by

$$U(t) = \sum_{m=0}^{M} |m\rangle\langle m| \exp(-iE_m t),$$

Quantum dynamics

One can investigate the quantum dynamics of the Hamiltonian in the absence of the external potential ($\Delta\mu = 0$) using the exact diagonalization method.
The time evolution of any state is determined by

$$|\Psi(t)\rangle = U(t)|\phi_0\rangle,$$

where U is the temporal evolution operator given by

$$U(t) = \sum_{m=0}^{M} |m\rangle\langle m| \exp(-iE_m t),$$

$|m\rangle$ is an eigenstate with energy E_m and $|\phi_0\rangle$ represents the initial state.

Quantum dynamics

One can investigate the quantum dynamics of the Hamiltonian in the absence of the external potential ($\Delta\mu = 0$) using the exact diagonalization method.
The time evolution of any state is determined by

$$|\Psi(t)\rangle = U(t)|\phi_0\rangle,$$

where U is the temporal evolution operator given by

$$U(t) = \sum_{m=0}^{M} |m\rangle\langle m| \exp(-iE_m t),$$

$|m\rangle$ is an eigenstate with energy E_m and $|\phi_0\rangle$ represents the initial state.Using these expressions we can compute the expectation value of the relative number of particles

Quantum dynamics

One can investigate the quantum dynamics of the Hamiltonian in the absence of the external potential ($\Delta\mu = 0$) using the exact diagonalization method.
The time evolution of any state is determined by

$$|\Psi(t)\rangle = U(t)|\phi_0\rangle,$$

where U is the temporal evolution operator given by

$$U(t) = \sum_{m=0}^{M} |m\rangle\langle m| \exp(-iE_m t),$$

$|m\rangle$ is an eigenstate with energy E_m and $|\phi_0\rangle$ represents the initial state.Using these expressions we can compute the expectation value of the relative number of particles

$$\langle (N_1 - N_2)(t)\rangle = \langle \Psi(t)|N_1 - N_2|\Psi(t)\rangle. \tag{8}$$

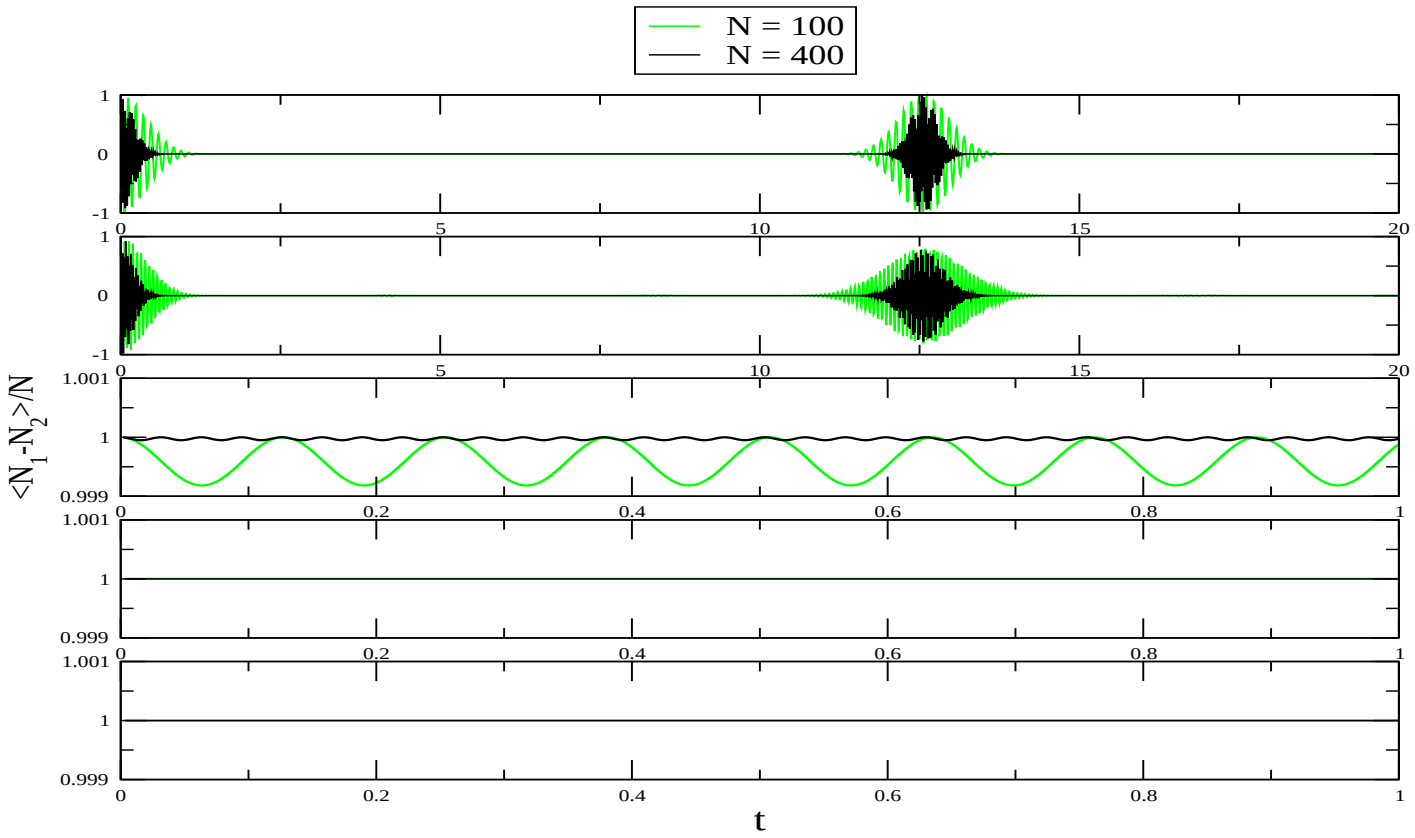

Figure: Time evolution of the expectation value for the relative number of particles for different ratios of the coupling $k/\mathcal{E}_{\mathcal{J}}$ from the top (Rabi regime) to the bottom (Fock regime): $k/\mathcal{E}_{\mathcal{J}} = 1/N^2, 1/N, 1, N, N^2$ for $N = 100, 400$ and the initial state is $|N, 0\rangle$.

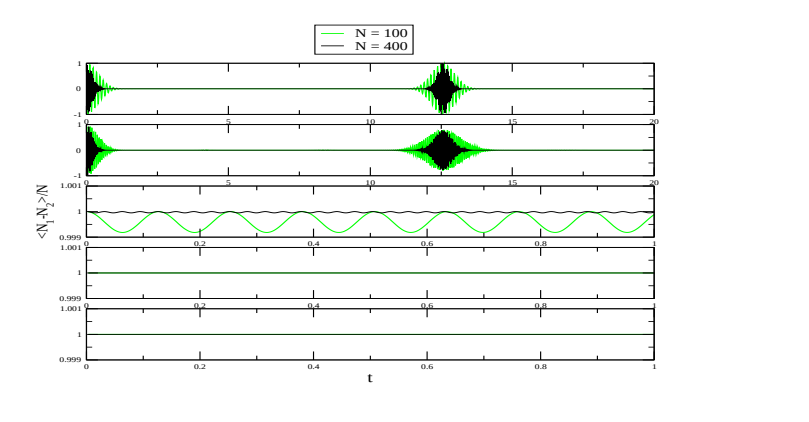

One can see that the qualitative behaviour in each region does not depend on the number of particles.

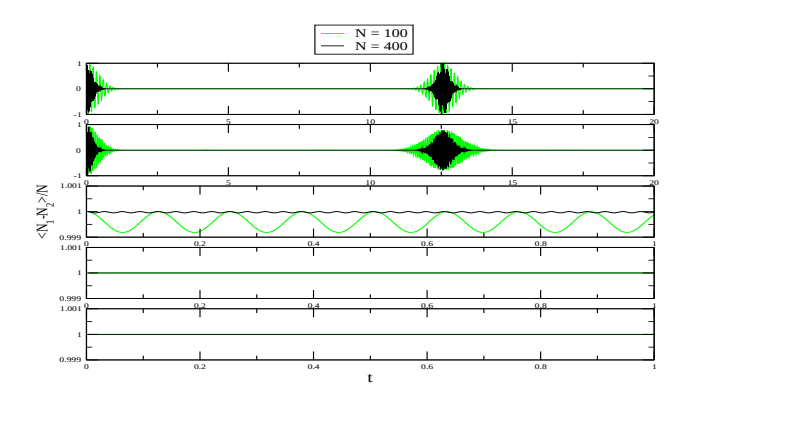

One can see that the qualitative behaviour in each region does not depend on the number of particles.
In the interval $k/\mathcal{E}_{\mathcal{J}} \in [1/N^2, 1/N]$ (close to the Rabi regime) the collapse and revival time takes the constant value $t_{cr} = 4\pi$ The ratio $k/\mathcal{E}_{\mathcal{J}} = 1/N^2$ means that we are using $k = 1$ and $\mathcal{E}_{\mathcal{J}} = N^2$ and similarly for the other cases.

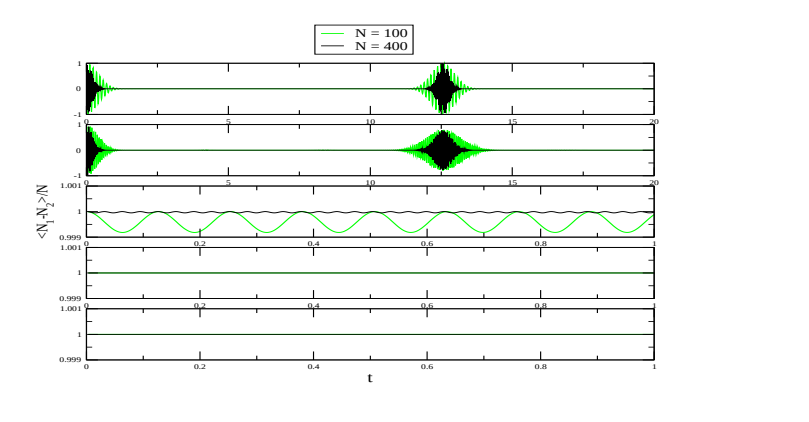

One can see that the qualitative behaviour in each region does not depend on the number of particles.
In the interval $k/\mathcal{E}_{\mathcal{J}} \in [1/N^2, 1/N]$ (close to the Rabi regime) the collapse and revival time takes the constant value $t_{cr} = 4\pi$ The ratio $k/\mathcal{E}_{\mathcal{J}} = 1/N^2$ means that we are using $k = 1$ and $\mathcal{E}_{\mathcal{J}} = N^2$ and similarly for the other cases.
In the interval between $k/\mathcal{E}_{\mathcal{J}} = 1/N$ and $k/\mathcal{E}_{\mathcal{J}} = 1$ the system undergoes a transition from oscillations which vary between positive and negative values of $\langle N_1 - N_2 \rangle$ (delocalized) to one where $\langle N_1 - N_2 \rangle$ is close to N (self-trapping).

Now we focus in more detail the time evolution of the expectation value of the relative number of particles in the interval $k/\mathcal{E}_{\mathcal{J}} \in [1/N, 1]$

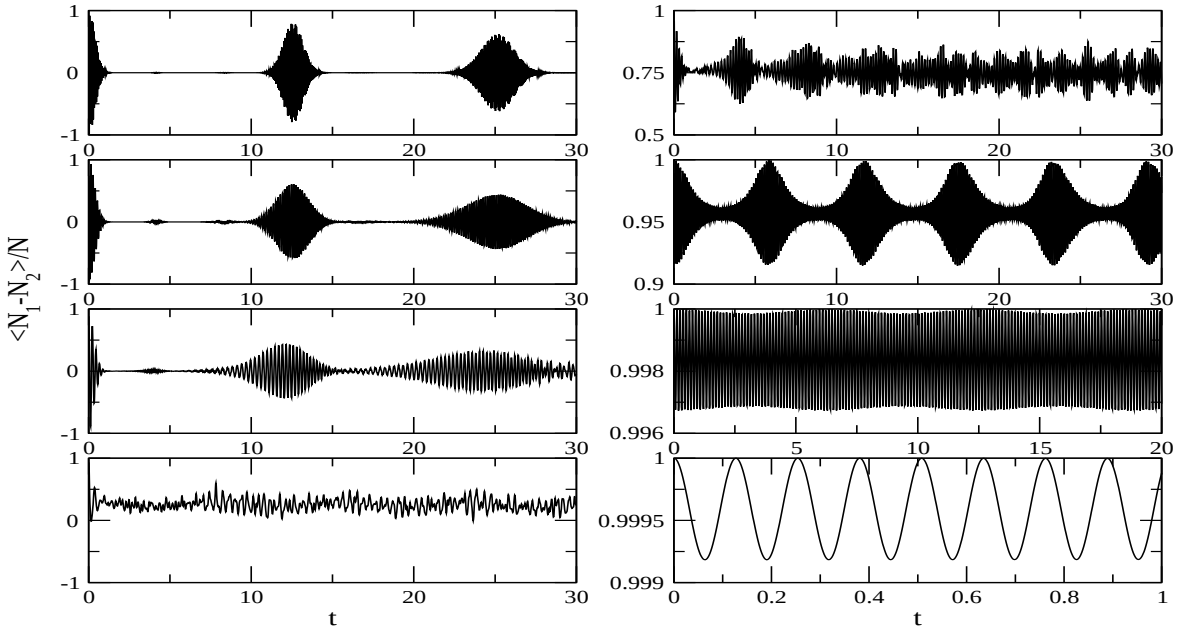

Figure: Time evolution of the expectation value between $k/\mathcal{E}_{\mathcal{J}} = 1/N$ and $k/\mathcal{E}_{\mathcal{J}} = 1$. On the left, from the top to the bottom $k/\mathcal{E}_{\mathcal{J}} = 1/N, 2/N, 3/N, 4/N$ and on the right, from the top to the bottom $k/\mathcal{E}_{\mathcal{J}} = 5/N, 10/N, 50/N, 1$, where $N = 100$ and the initial state is $|N, 0\rangle$.

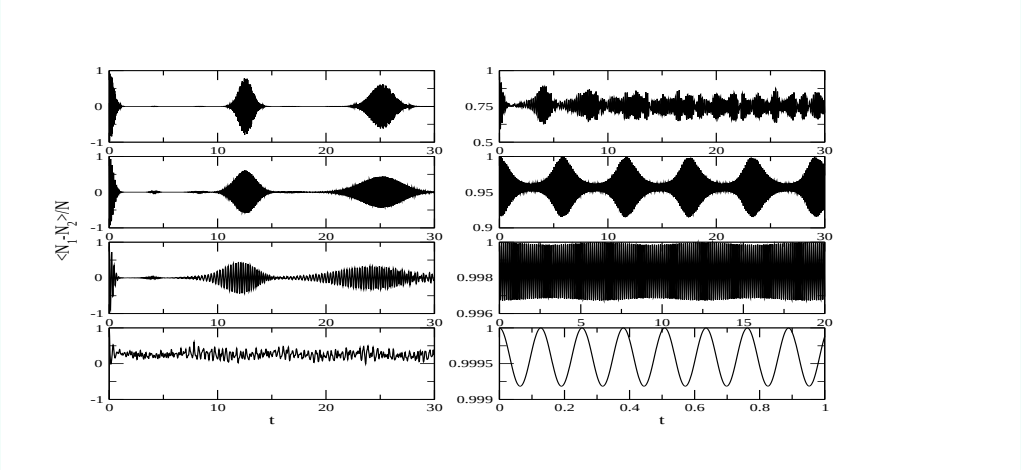

$N = 100$: we observe the evolution of the dynamics from a collapse and revival sequence for $k/\mathcal{E}_{\mathcal{J}} < 4/N$,

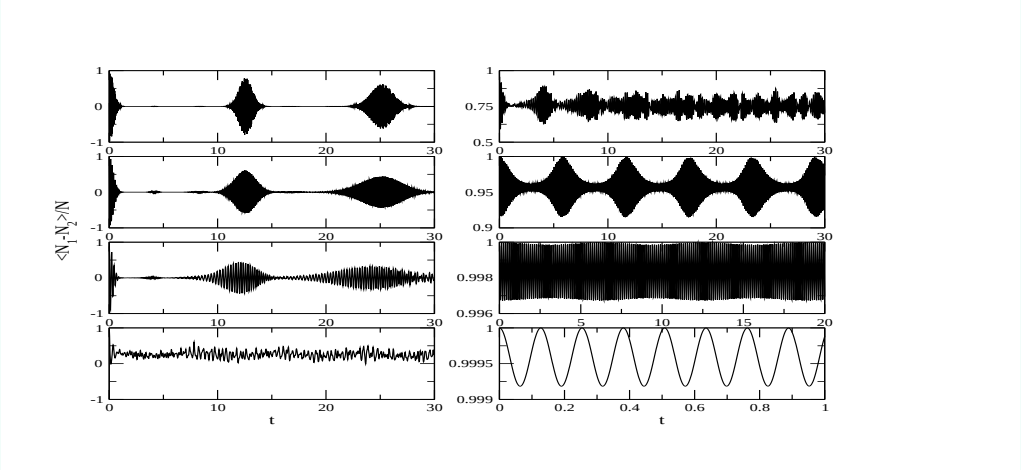

$N = 100$: we observe the evolution of the dynamics from a collapse and revival sequence for $k/\mathcal{E}_{\mathcal{J}} < 4/N$, through the self-trapping transition at $k/\mathcal{E}_{\mathcal{J}} = 4/N$,

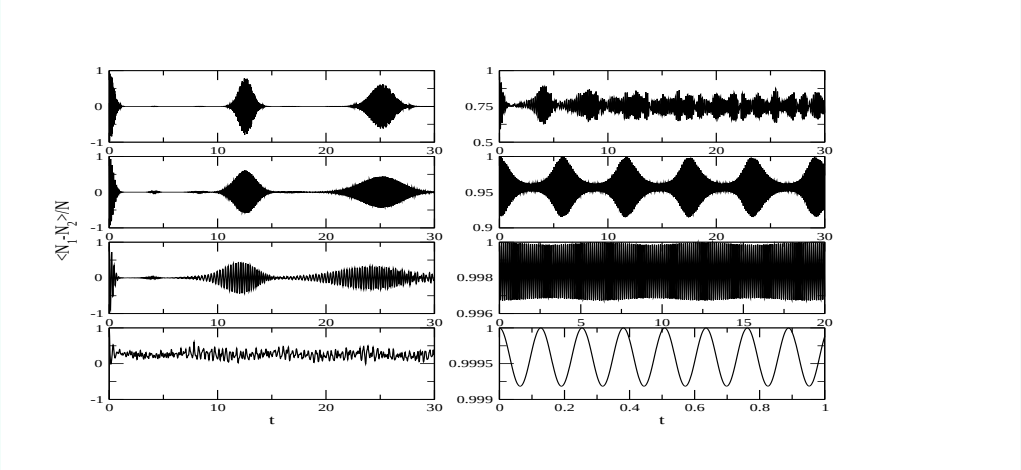

$N = 100$: we observe the evolution of the dynamics from a collapse and revival sequence for $k/\mathcal{E}_{\mathcal{J}} < 4/N$, through the self-trapping transition at $k/\mathcal{E}_{\mathcal{J}} = 4/N$, and toward small amplitude harmonic oscillations in the imbalance of the localized state when $k/\mathcal{E}_{\mathcal{J}} = 1$.

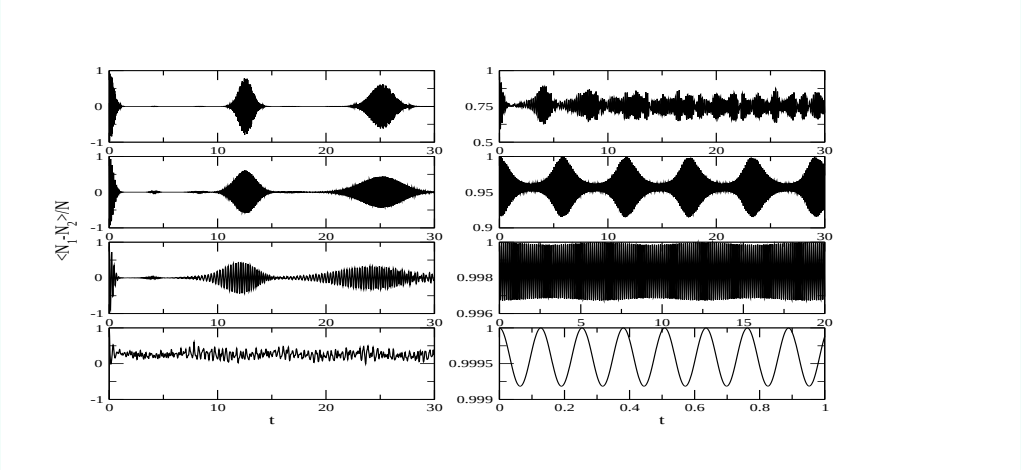

$N = 100$: we observe the evolution of the dynamics from a collapse and revival sequence for $k/\mathcal{E}_{\mathcal{J}} < 4/N$, through the self-trapping transition at $k/\mathcal{E}_{\mathcal{J}} = 4/N$, and toward small amplitude harmonic oscillations in the imbalance of the localized state when $k/\mathcal{E}_{\mathcal{J}} = 1$. In the localized phase $k/\mathcal{E}_{\mathcal{J}} > 4/N$ one also observes the re-emergence of a collapse and revival sequence.

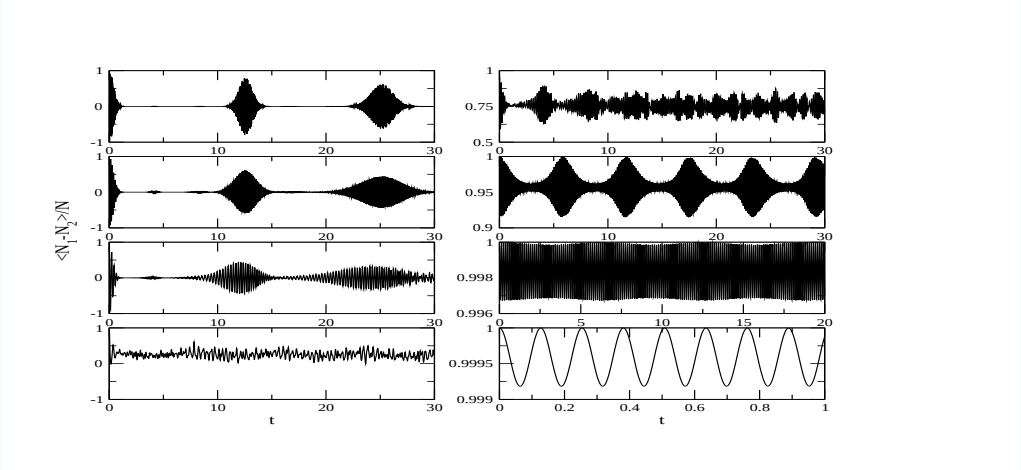

$N = 100$: we observe the evolution of the dynamics from a collapse and revival sequence for $k/\mathcal{E}_{\mathcal{J}} < 4/N$, through the self-trapping transition at $k/\mathcal{E}_{\mathcal{J}} = 4/N$, and toward small amplitude harmonic oscillations in the imbalance of the localized state when $k/\mathcal{E}_{\mathcal{J}} = 1$. In the localized phase $k/\mathcal{E}_{\mathcal{J}} > 4/N$ one also observes the re-emergence of a collapse and revival sequence.Further increases in $k/\mathcal{E}_{\mathcal{J}}$ lead to a decaying of the collapse and revival sequence toward harmonic oscillations which occur at $k/\mathcal{E}_{\mathcal{J}} = 1$.

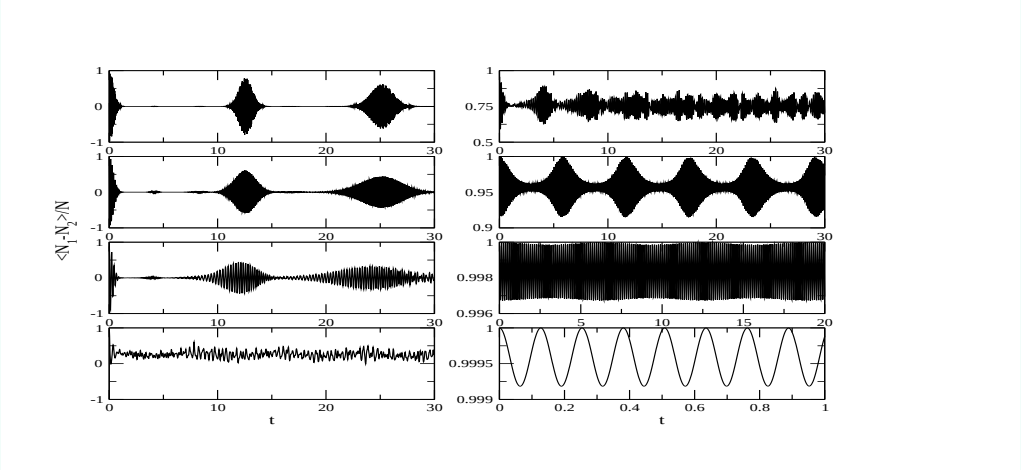

$N = 100$: we observe the evolution of the dynamics from a collapse and revival sequence for $k/\mathcal{E}_{\mathcal{J}} < 4/N$, through the self-trapping transition at $k/\mathcal{E}_{\mathcal{J}} = 4/N$, and toward small amplitude harmonic oscillations in the imbalance of the localized state when $k/\mathcal{E}_{\mathcal{J}} = 1$. In the localized phase $k/\mathcal{E}_{\mathcal{J}} > 4/N$ one also observes the re-emergence of a collapse and revival sequence.Further increases in $k/\mathcal{E}_{\mathcal{J}}$ lead to a decaying of the collapse and revival sequence toward harmonic oscillations which occur at $k/\mathcal{E}_{\mathcal{J}} = 1$.
From the above picture it is clear that the threshold coupling $k/\mathcal{E}_{\mathcal{J}} = 4/N$ predicted by the classical analysis, representing the boundary between a delocalized evolution ($k/\mathcal{E}_{\mathcal{J}} < 4/N$) and self-trapped evolution ($k/\mathcal{E}_{\mathcal{J}} > 4/N$), also holds for the quantum dynamics.

Algebraic Bethe ansatz solution

Here we will look into the exact Bethe ansatz solution of (1) revising some of the concepts discussed in previous lectures.
We begin with the $su(2)$-invariant R-matrix, depending on the spectral parameter u:

Algebraic Bethe ansatz solution

Here we will look into the exact Bethe ansatz solution of (1) revising some of the concepts discussed in previous lectures.
We begin with the $su(2)$-invariant R-matrix, depending on the spectral parameter u:

$$R(u) = \begin{pmatrix} 1 & 0 & 0 & 0 \\ 0 & b(u) & c(u) & 0 \\ 0 & c(u) & b(u) & 0 \\ 0 & 0 & 0 & 1 \end{pmatrix}, \tag{9}$$

with $b(u) = u/(u+\eta)$ and $c(u) = \eta/(u+\eta)$. Above, η is an arbitrary parameter, to be chosen later. $R(u)$ satisfies the Yang–Baxter equation

$$R_{12}(u-v)R_{13}(u)R_{23}(v) = R_{23}(v)R_{13}(u)R_{12}(u-v). \tag{10}$$

Here $R_{jk}(u)$ denotes the matrix acting non-trivially on the j-th and k-th spaces and as the identity on the remaining space.

Next we define the Yang–Baxter algebra $T(u)$,

$$T(u) = \begin{pmatrix} A(u) & B(u) \\ C(u) & D(u) \end{pmatrix} \tag{11}$$

subject to the constraint

$$R_{ab}(u-v)T_a(u)T_b(v) = T_b(v)T_a(u)R_{ab}(u-v). \tag{12}$$

We may choose the following realization for the Yang–Baxter algebra

$$\pi(T_a(u)) = L_{a1}(u+\omega)L_{a2}(u-\omega), \tag{13}$$

written in terms of the L operators

$$L_i(u) = \begin{pmatrix} u+\eta N_i & b_i \\ b_i^\dagger & \eta^{-1} \end{pmatrix} \qquad i = 1, 2. \tag{14}$$

Explicitly,

$$\pi(T_a(u)) = \begin{pmatrix} (u+\omega+\eta N_1)(u-\omega+\eta N_2) + b_2^\dagger b_1 & (u+\omega+\eta N_1)b_2 + \eta^{-1} b_1 \\ (u-\omega+\eta N_2)b_1^\dagger + \eta^{-1} b_2^\dagger & b_1^\dagger b_2 + \eta^{-2} \end{pmatrix} \tag{15}$$

Since $L(u)$ satisfies the RLL relation it is easy to check that the Yang-Baxter algebra (12) is also obeyed.

Each entry of the Monodromy T is an operator

$$A(u) = (u + \omega + \eta N_1)(u - \omega + \eta N_2) + b_2^\dagger b_1 \tag{16}$$

$$B(u) = (u + \omega + \eta N_1) b_2 + \eta^{-1} b_1 \tag{17}$$

$$C(u) = (u - \omega + \eta N_2) b_1^\dagger + \eta^{-1} b_2^\dagger \tag{18}$$

$$D(u) = b_1^\dagger b_2 + \eta^{-2} \tag{19}$$

From the Yang Baxter algebra one sees that they satisfy relations,

$$[A(u), A(v)] = [D(u), D(v)] = [B(u), B(v)] = [C(u), C(v)] = 0 \tag{20}$$

$$A(u)C(v) = \frac{u - v + \eta}{u - v} C(v)A(u) - \frac{\eta}{u - v} C(u)A(v) \tag{21}$$

$$D(u)C(v) = \frac{u - v - \eta}{u - v} C(v)D(u) + \frac{\eta}{u - v} C(u)D(v) \tag{22}$$

A key step in applying the algebraic Bethe ansatz approach is finding a suitable pseudovacuum state, $|0\rangle$, such that

$$A(u)|0\rangle = a(u)|0\rangle \tag{23}$$
$$B(u)|0\rangle = 0 \tag{24}$$
$$C(u)|0\rangle \neq 0 \tag{25}$$
$$D(u)|0\rangle = d(u)|0\rangle \tag{26}$$

where here $a(u)$ and $d(u)$ are scalar functions. We will choose as pseudovacuum the Fock vacuum state annihilated by the operators b_i as it also satisfies

$$B(u)|0\rangle = [(u+\omega+\eta N_1)b_2 + \eta^{-1}b_1]|0\rangle$$

Now

$$A(u)|0\rangle = [(u+\omega+\eta N_1)(u-\omega+\eta N_2) + b_2^\dagger b_1]|0\rangle = (u+\omega)(u-\omega)|0\rangle$$

and

$$D(u)|0\rangle = [b_1^\dagger b_2 + \eta^{-2}]|0\rangle = \eta^{-2}|0\rangle$$

The next step is the choice of the Bethe state

$$|\vec{v}\rangle \equiv |v_1, ..., v_M\rangle = \prod_{i=1}^{M} C(v_i)\,|0\rangle\,. \tag{27}$$

Note that because $[C(u),\ C(v)] = 0$, the ordering is not important in the product of (27). The methodology of the algebraic Bethe ansatz is to to determine the action of $t(u)$ on $|\vec{v}\rangle$ using the commutation relations Eqs.(20-22).

Exercise:

1- Find the Bethe ansatz equations for the 2-site B-H model.

2- Find, numerically, the roots of the BAE for the ground state, for different values of the parameters.